

Research Report

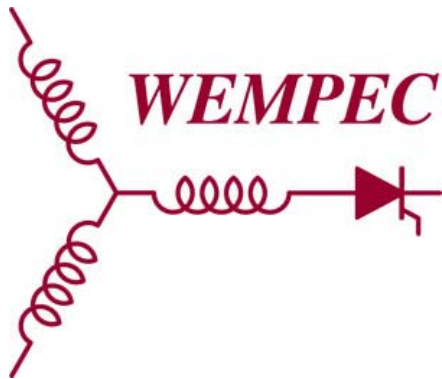
2014-28

**Optimal Design of Ultra-High Speed Axial Flux Permanent Magnet Motor with  
Sinusoidal Back-EMF**

**S. Kumar, W. Zhao, T.A. Lipo\*, B. Kwon**

Department of Electronic Systems  
Engineering,  
Hanyang University,  
Ansan-si, Gyeonggi-do, 426-791, Korea

\* Department of Electrical and Computer  
Engineering,  
University of Wisconsin-Madison,  
Madison, WI, 53706-1691, USA



**Wisconsin  
Electric  
Machines &  
Power  
Electronics  
Consortium**

University of Wisconsin-Madison  
College of Engineering  
Wisconsin Power Electronics Research Center  
2559D Engineering Hall  
1415 Engineering Drive  
Madison WI 53706-1691

© Confidential

정현파의 역기전력을 갖는 초고속 축방향 자속형 영구자석 모터의 최적 설계

수닐 쿠마르\*, 조문량\*, Thomas Anthony Lipo\*\*, 권병일\*  
 한양대학교\*, 위스콘신-메디슨 대학교\*\*

Optimal Design of Ultra-High Speed Axial Flux Permanent Magnet Motor with Sinusoidal Back-EMF

Sunil Kumar\*, Wenliang Zhao\*, Thomas Anthony Lipo\*\*, Byung-II Kwon\*  
 \*Hanyang University, \*\*University of Wisconsin-Madison

**Abstract** - This paper focuses on the optimal design of rotor pole shape of a small size, very high speed axial flux PM motor. The target is to achieve sinusoidal back-EMF, thus reduce cogging torque and torque ripple of the machine. This is very crucial for the performance and smooth running of the machine. For optimization, Kriging method based on Latin Hypercube Sampling (LHS) and Genetic Algorithm (GA) are employed. Both no-load and full-load conditions are analyzed by 3-D Finite Element Method (FEM) and the results are then evaluated and compared with the basic model.

1. Introduction

The use of small and very high speed electric machines has been an area of interest for many applications, particularly in aerospace flywheel energy storage systems which need the machine to operate at extremely high speed; i.e., of the order of hundreds of thousands of revolutions per minute (rpm) [1]. At such high speed, the machine performance should be carefully investigated such as cogging torque and torque ripple; to ensure smooth operation. For these reasons, the machine should have sinusoidal back-EMF since the cogging torque and torque ripple largely depends upon the harmonics present in the back-EMF waveform of the machine [2].

In this paper, the rotor pole shape is designed for a two phase axial flux permanent magnet (AFPM) motor rotating at one million rpm to get sinusoidal back-EMF. The basic model is shown in Fig. 1, which is double-rotor-single-stator design.

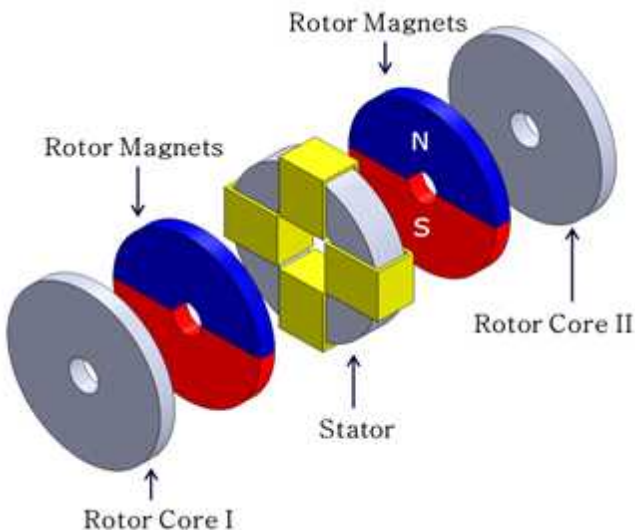


Fig. 1. Basic model showing different parts

The stator is composed of single turn coils with two coils per phase distributed over the stator periphery. The rotors comprise of two pole permanent magnet structure. Firstly, a mathematical equation driven rotor pole shape is proposed and 3-D FEM analysis is performed. With this proposed design, the rotor pole is then further optimized using Kriging method and Genetic Algorithm [3].

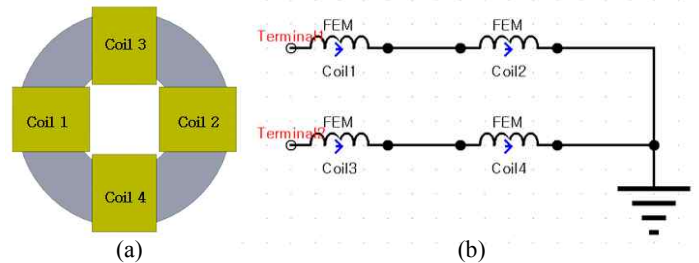


Fig. 2.(a) Stator core and coils (b) equivalent circuit diagram

2. Design

2.1 Stator

The stator consists of a slotless cylindrical ferrite core. The core is wound by four single turn copper coils forming two coils for each phase as shown in Fig. 2. Table I shows the dimensions used in the machine design.

<Table I> Machine Dimensions

Item	Unit	Value
Stator Outer Diameter	mm	50
Stator Inner Diameter	mm	24
Rotor Outer Diameter	mm	52
Rotor Inner Diameter	mm	10
Air gap between rotor magnet and stator coil	mm	0.5
Rotor Core Thickness	mm	5
Magnet Thickness	mm	5
Stator Core Thickness	mm	10
Coil Thickness	mm	1
Coil Height	mm	18
Coil Width	mm	15
Clearance between Stator coil and Stator Core	mm	0.1
Number of Phases	-	2
Number of Turns per coil	-	1
Peak Current Density	A/mm <sup>2</sup>	10
Rotor Angular Speed	rpm	1,000,000

## 2.2 Rotor

The design comprises of two symmetrical rotors on both sides of the stator. Each rotor consists of one ferrite core and two permanent magnets as rotor poles. NdFeB (Hitachi Metals NEOMAX-42) is used as magnet material due to its high energy density [4]. In basic model, the magnets completely fill the rotor which makes the magnet shape a half circle. While in proposed model, the magnet's outer surface is used as a design variable.

## 2.3 Proposed Model

In proposed model, only rotor magnet shape is designed using the mathematical derivation. Consider the voltage induced in a rotating wire of length  $R_0$  on an x-y plane in a magnetic field whose magnitude is constant and directed in the z-direction. In polar coordinates, the field of a value 'B' exists between  $0 < r < R_0$  and is zero when  $r > R_0$ . The voltage induced in the spinning wire segment is the vector equation:

$$E(t) = \int_0^R (\vec{v} \times \vec{B}) \cdot \vec{dr}$$

Where,  $\vec{v}$  is the velocity directed in the circumferential direction,  $\vec{B}$  is the flux density in the z-direction and  $\vec{dr}$  is an incremental length of the work oriented in the radial direction. Upon taking the cross and dot products and noting that the flux density is zero beyond the value  $R$ ,

$$E(t) = B \int_0^R v dr$$

The velocity of a particular value of winding segment is  $v = r\omega$ . Where,  $\omega$  is angular velocity of the rotating wire segment. The induced voltage  $E$  is therefore,

$$E(t) = \omega B \int_0^R r dr = \omega B \frac{R^2}{2}$$

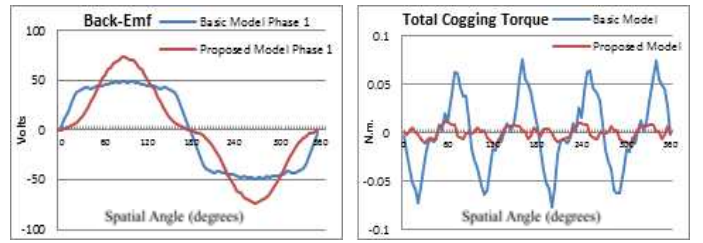
Assume now, if  $B$  is a constant value but is distributed over the region of the polar surface such that:

$$R = R_0 \sqrt{\sin\theta} \quad (1)$$

Where,  $\theta$  is the angular measure in the polar coordinate system. Then,

$$E(t) = \frac{\omega B R_0^2}{2} \sin\theta$$

in which case the EMF varies sinusoidally. A plot of the required magnet shape based on equation (1) is shown in Fig. 3 (a).



(a) Back-EMF

(b) Cogging Torque

Fig. 4. Comparison of Basic and Proposed Model at no-load.

As shown in the results, the cogging torque has been greatly reduced but the back-EMF is distorted from the sinusoidal waveform. This is mainly due to the fact that the winding has been represented by a line with no width. In order to compensate this effect, the magnet shape needs to be increased in a similar fashion which is discussed in the next section.

## 3. Optimization

The optimization process flow-chart is shown in Fig. 5. In this optimization process, one more equation driven curve is introduced to increase the magnet size. To perform this, equation (1) has been transformed into parametric form as shown below:

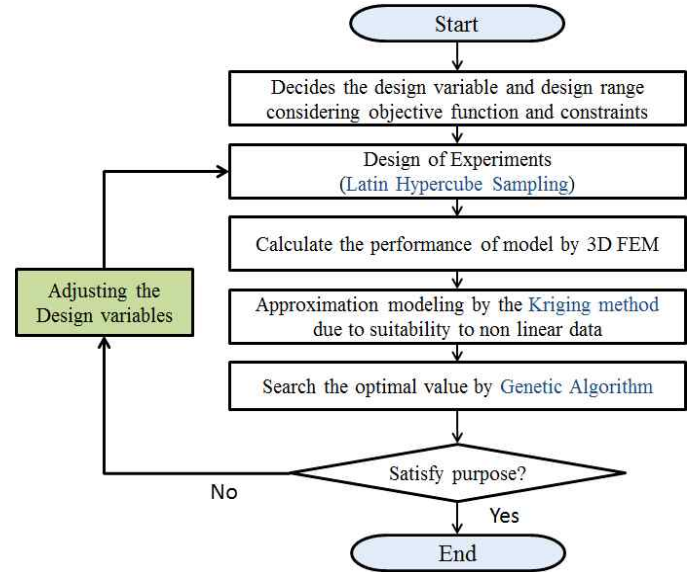


Fig. 5. Optimization Process Flow

Since we know,  $x = R\cos\theta$  and  $y = R\sin\theta$ . Substituting the value of  $R$  from equation (1) we have,

$$x = R_0 \sqrt{\sin\theta} \cos\theta \quad \text{and,}$$

$$y = R_0 \sqrt{\sin\theta} \sin\theta$$

The constant  $R_0$  is the maximum value of  $y$  at  $\theta = \pi/2$  and is equal to the radius of the rotor in case of proposed model. In order to insert another curve, we need design variable which changes the shape of the magnet over the rotor area. It is noted that by assigning  $R_0$  into variable we can successfully adjust the magnet shape. The final magnet shape will be the outer boundaries of the initial proposed curve and this variable curve. The above equations then changes to:

$$x = X_0 \sqrt{\sin\theta} \cos\theta \quad \text{and,}$$

$$y = Y_0 \sqrt{\sin\theta} \sin\theta$$

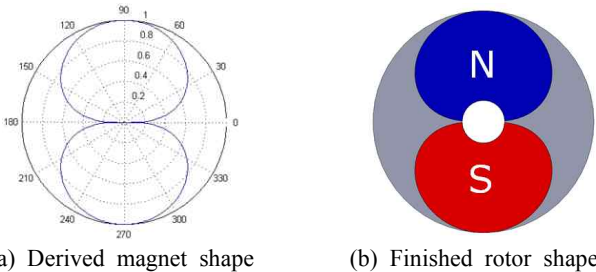


Fig. 3. Proposed rotor shape

## 2.4 Simulation Results

The no-load analysis has been carried out using 3-D FEM simulation in JMAG® Designer software to compare the basic and proposed model. The no-load voltage induced in the stator windings, or the back-EMF, and the total cogging torque (Sum of Rotor I torque and Rotor II torque) has been plotted in Fig. 4.

Fig. 6. shows the variables  $X_0$  and  $Y_0$  and the corresponding magnet shape. These variables adjust the shape of the variable curve.

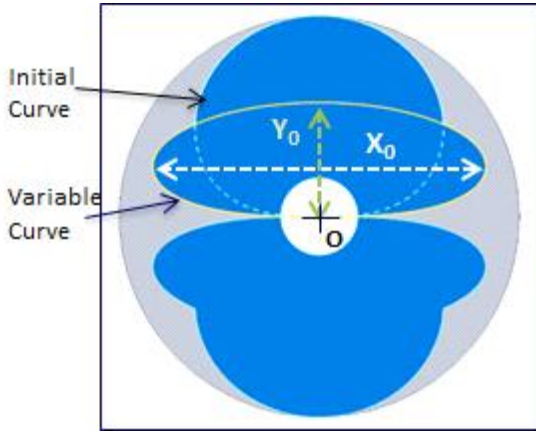


Fig. 6. Optimization variables for rotor magnet shape

The objective functions, design variables and constraint are shown below:

- ❖ Objective function
  - Minimize THD of Back-EMF
  - Minimize Cogging Torque
- ❖ Design variables
  - $28 \text{ mm} \leq X_0 \leq 38 \text{ mm}$
  - $02 \text{ mm} \leq Y_0 \leq 24 \text{ mm}$
- ❖ Constraint
  - Magnet volume per pole  $\leq 5309 \text{ mm}^3$

The range of design variables is selected in such a way that the magnet boundary should remain outside of the initial curve and well inside the rotor area [5].

In design of experiments, twenty number of samples have been generated using Latin Hypercube Sampling method for the design variables. 3-D FEM no-load analysis is carried out for all the samples to calculate THD of back-EMF and peak-to-peak cogging torque. Kriging method optimization and Genetic Algorithm are employed to get the optimal values and finally the optimal results are verified by FEM results. Final optimal values obtained in this procedure are:

- $X_0 = 32.377 \text{ mm}$
- $Y_0 = 20.755 \text{ mm}$

#### 4. Results

Fig.7. shows the simulation results of the basic, proposed and the optimized model. The back-EMF waveform of the optimized model is found to be more sinusoidal, the cogging torque is considerably reduced, while the electromagnetic torque has very much reduced ripples. This shows that the machine performance has been greatly improved in terms of cogging torque and torque ripple.

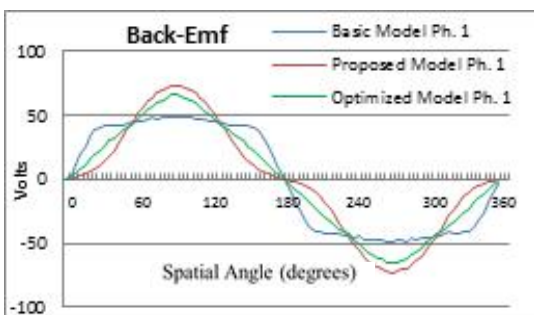


Fig. 7 (a). Back-EMF of phase I

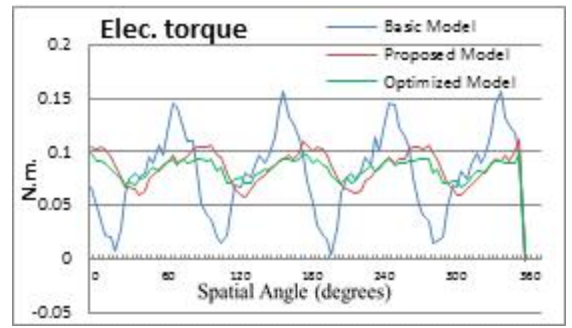


Fig. 7 (b). Total Torque Ripple (Rotor I + Rotor II)

Table II shows the performance comparison of all the models. The torque values are the sum of Rotor-I torque and Rotor-II torque.

<Table II> Performance Comparison

Results	Unit	Basic Model	Proposed Model	Optimized Model
Back-EMF (THD)	%	22.38	24.79	8.48
Back-EMF (RMS)	Volts	40.62	43.58	41.64
Cogging Torque (pk-pk)	Nm	0.1524	0.0233	0.0233
Elec. Torque (Average)	Nm	0.0803	0.0855	0.0842
Torque Ripple	%	190.62	61.59	38.38

#### 5. Conclusion

A small size and ultra-high speed AFPM motor has been introduced in this paper to improve its performance. The rotor magnet shape is used as a design domain to reduce the back-EMF THD and cogging torque of the machine. The 3-D FEM simulation results show that the optimized model has much lower values of back-EMF THD, cogging torque and torque ripple than the basic model. In future, more work will be done to get the best results and a smooth magnet shape is formed from the manufacturing point of view.

This research was supported by BK21PLUS program through the National Research Foundation of Korea funded by the Ministry of Education.

#### [References]

- [1] Wensen Wang; Hofmann, H.; Bakis, C.E., "Ultrahigh Speed Permanent Magnet Motor/Generator for Aerospace Flywheel Energy Storage Applications," *Electric Machines and Drives, 2005 IEEE International Conference on*, vol., no., pp.1494,1500, 15-15 May 2005.
- [2] Shah, S.Q.A.; Lipo, T.A.; Byung-il Kwon, "Modeling of Novel Permanent Magnet Pole Shape SPM Motor for Reducing Torque Pulsation," *Magnetics, IEEE Transactions on*, vol.48, no.11, pp.4626,4629, Nov. 2012
- [3] Yong-min You; Hai Lin; Byung-il Kwon, "Optimal Design of a Distributed Winding Type Axial Flux Permanent Magnet Synchronous Generator," *Journal of Electrical Engineering and technology*, Vol. 7, No. 1, pp. 69-74, 2012.
- [4] Zheng, L.; Wu, T.X.; Sundaram, K.B.; Vaidya, J.; Zhao, L.; Acharya, D.; Ham, C.H.; Kapat, J.; Chow, L., "Analysis and Test of a High-Speed Axial Flux Permanent Magnet Synchronous Motor," *Electric Machines and Drives, 2005 IEEE International Conference on*, vol., no., pp.119,124, 15-15 May 2005.
- [5] Jin-hee Lee; Byung-il Kwon, "Optimal Rotor Shape Design of a Concentrated Flux IPM-Type Motor for Improving Efficiency and Operation Range," *Magnetics, IEEE Transactions on*, vol.49, no.5, pp.2205,2208, May 2013.